

## STUDY OF HOLE-BLOCKING AND ELECTRON-BLOCKING LAYERS IN A InAs/GaAs MULTIPLE QUANTUM-WELL SOLAR CELL

Sobhan Abbasian<sup>1,2</sup>, Reza Sabbaghi-Nadooshan<sup>1</sup>

<sup>1</sup>Electrical Engineering Department, Islamic Azad University, Central Tehran Branch, Tehran, Iran

<sup>2</sup>Alborz Electricity Distribution Company, Karaj, Iran

**Abstract.** *In this work, a GaAs-based quantum well solar cell with a 25-layer InAs/GaAs intermediate layer is simulated in Silvaco Atlas TCAD software. In order to reduce the recombination caused by the presence of the quantum layers and increase the absorption of photons, electron blocking layers (EBLs) and hole blocking layers (HBLs) have been added to the solar cell in an  $In_{0.5}(Al_{0.7}Ga_{0.3})_{0.5}P$  semiconductor. The results show that the efficiency of the proposed solar cell increases 17.38% by obtaining impurity the thickness and doping of the EBL and HBL layers. It can be concluded that the use of the  $In_{0.5}(Al_{0.7}Ga_{0.3})_{0.5}P$  semiconductor with EBL and HBL layers decreases the open circuit voltage ( $V_{oc}$ ) caused in the quantum wells. The efficiency of the proposed solar cell with EBL and HBL layers was found to be 44.65%.*

**Key words:** *Electron-blocking Layers, hole-blocking Layers, InAs/GaAs, Quantum-well Solar Cell*

### 1. INTRODUCTION

The increasing human need for energy has drawn the attention of many researchers to renewable energy. Solar cells are a clean energy source that absorb and convert solar energy into electricity. Much research has been done on solar cells with semiconductors from the III-V group because of their high efficiency. Barnham et al. improved quantum solar cell function by inserting a quantum well as the middle layer in a p-i-n cell [1]. Paxman et al. found that the density of the optical current and conversion efficiency increased in p-i-n structures with GaAs/AlGaAs quantum wells [2]. In fact, a quantum well in the intermediate layer produces an additional electron-hole pair by absorption of photons with less energy and improves the spectral response by absorbing different energy photons. The increase in the shortcircuit current ( $J_{sc}$ ) increases absorption, but the increase in the recombination of carriers in the quantum well causes  $V_{oc}$  to decrease [2-

---

Received February 7, 2020; received in revised form June 14, 2020

**Corresponding author:** Reza Sabbaghi-Nadooshan  
Niayesh Building, Emam Hasan Blvd., Pounak, Tehran, Iran  
E-mail: [r\\_sabbaghi@iauctb.ac.ir](mailto:r_sabbaghi@iauctb.ac.ir)

3]. An EBL layer with a band gap larger than the p-n junction in the solar cell creates an electric field and prevents reconciliation of carrier density [4-5]. Therefore, the EBL and HBL layers cause an increase the  $J_{sc}$  without reducing the  $V_{oc}$  and increasing the gain in the p-i-n solar cells. In 2015, Feroz Ali et al achieved a 26.285% efficiency in Si solar cell by designing an EBL layer with 2.1eV bandwidth [6]. Denis et al showed in 2010 that InAs /GaAs quantum dot cells increase photon absorption [7]. Peter James et al then designed a GaSb/GaAs quantum dot cell in 2011 [8]. Wei-Sheng designed an InAs/GaAsSb quantum dot in 2012 to increase short-circuit current by 8.8% [9]. In 2013, Xiaoguang et al achieved 17% efficiency by investigating the effects of Si-doping on InAs/GaAs quantum dots [10]. The effect of electric field on different layers of InAs/GaAs quantum dots was investigated by Yushuai et al in 2014 [11]. In 2015, Inigo et al designed the InAs/InGaP Quantum-Dot cell [12]. Utrilla et al increased the range of InAs/GaAs quantum dots in 2016 using semiconductors in InAs/GaAs cells [13]. An analytical study on InAs/GaAs quantum dots solar cells was conducted in 2017 by Sayantan et al [14]. In 2018, they conducted studies on the optical properties of InAs/GaAs quantum dots cells [15]. The effects of temperature on InAs/GaAs quantum dots were investigated by Abdelkader et al in 2019 [16].

The present study was undertaken to simulate a GaAs/InAs multi-quantum well solar cell using Silvaco Atlas TCAD software [17]. As can be seen in [18], the BSF layer of the semiconductor  $In_{0.5}(Al_{0.7}Ga_{0.3})_{0.5}P$  enhances the adsorption of charge carriers and promotes the solar cell yield. The proposed solar cell simulation confirms the increase efficiency with experimental results compared in this paper. In the present article, we used the EBL and HBL layer, which is similar in performance to BSF, and improved it via semiconductor  $In_{0.5}(Al_{0.7}Ga_{0.3})_{0.5}P$ . The efficiency of the solar cell of the addition of the  $In_{0.5}(Al_{0.7}Ga_{0.3})_{0.5}P$  semiconductor as the EBL and HBL layers is examined. The EBL layer (0.05  $\mu m$  in thickness; doping  $2 \times 10^{15} 1/cm^3$ ) and the HBL layer (2.0  $\mu m$  in thickness; doping of  $2 \times 10^{19} 1/cm^3$ ) increased solar cell efficiency 44.65%.

## 2. QUANTUM-WELL SOLAR CELL STRUCTURE

In a p-i-n solar cell, due to the presence of an intermediate band in the band gap ( $E_g$ ), the bandwidth of the conduction and valence bands absorbs more inlet photons. As shown in Fig. 1, the semiconductor band gap ( $E_g$ ) is divided into two smaller band gaps,  $E_L$  and  $E_H$ . Absorbing photons with less energy than the band gap ( $E_g$ ) leads to an increase in electron and hole production.

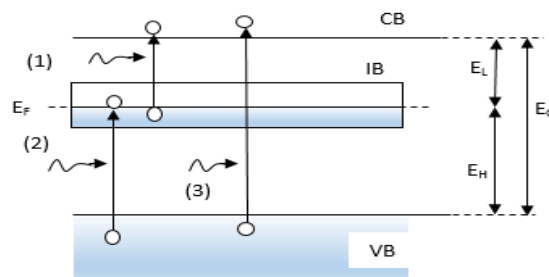


**Fig. 1** The photon absorption processes in structure of an intermediate band

To generate a pair of electron holes using photon absorption with less energy than the band gap ( $E_g$ ), an electron moves from the valence band to the middle band and places the hole in its bond. In the form of this transfer, the number 1 is displayed, and an electron from the midband to the conduction band is displayed with the number 2.

By absorbing photons with energy higher than the energy band gap ( $E_g$ ), the transfer of an electron from the valence band to the conduction band causes the normal production of the electron-hole to be coupled with the number 3 (as shown). To improve both transitions 1 and 2, the middle band is first filled with the electron. The middle band receiving electrons from the valence band to the middle band and electron transfer from the middle band to the conduction band [19].

Usually, longer wavelengths cannot direct the electron-hole generated in solar cells from the conduction band to the valence band because of low energy levels. In the intrinsic (i) region of a p-i-n solar cell, the quantum wells producing a pair of electrons and holes. As seen in Fig. 2, the electrons and holes produced in the quantum wells are released by heat and tunneling, and through the electric field in the p-i-n solar cell, they collide and move toward the contacts [20].

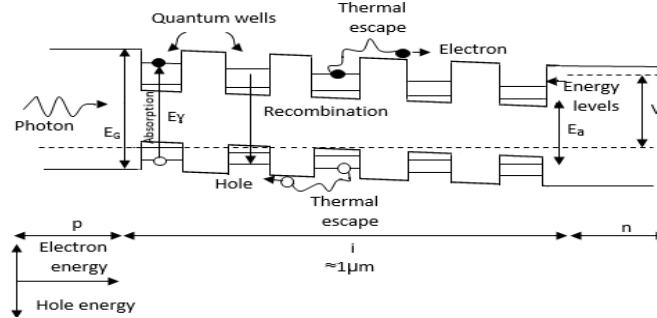


**Fig. 2** Quantum wells solar cell

### 3. MATERIALS SELECTION FOR DIFFERENT LAYERS

Table 1 shows the properties of the material for the various layers of the proposed cell. As shown in Table 1, the  $\text{In}_{0.49}\text{Ga}_{0.51}\text{P}$ , InAs and  $\text{In}_{0.5}(\text{Al}_{0.7}\text{Ga}_{0.3})_{0.5}\text{P}$  semiconductors prevent the recombination of electrons and holes by lattice matched to GaAs.

**Table 1** Major parameters for the ternary  $\text{In}_{0.49}\text{Ga}_{0.51}\text{P}$ , InAs and quaternary  $\text{In}_{0.5}(\text{Al}_{0.7}\text{Ga}_{0.3})_{0.5}\text{P}$  lattice matched to GaAs materials used in this design [21-25].

Material	GaAs	InGaP	InAlGaP	InAs
Band gap $E_g$ (eV) @300 K	1.42	1.9	2.3	0.36
Permittivity (es/eo)	13.1	11.6	11.7	15
Affinity (eV)	4.07	4.16	4.2	4.03
Heavy e- effective mass ( $m_e^*/m_0$ )	0.063	3	2.85	0.024
Heavy h + effective mass ( $m_h^*/m_0$ )	0.5	0.64	0.64	0.471
e- mobility $MUN$ ( $\text{cm}^2/\text{V}\times\text{s}$ )	8800	1945	2150	30000
h + mobility $MUP$ ( $\text{cm}^2/\text{V}\times\text{s}$ )	400	141	141	240
e- density of states $N_C$ ( $\text{cm}^{-3}$ )	$4.7\text{e}+17$	$1.30\text{e}+20$	$1.20\text{e}+20$	$8.7\text{e}+16$
h + density of states $N_V$ ( $\text{cm}^{-3}$ )	$7.0\text{e}+18$	$1.28\text{e}+19$	$1.28\text{e}+19$	$6.6\text{e}+18$

#### 4. MODELING PROCEDURES

##### 4.1. Cell structure

Figure 3 shows the structure of the proposed model. The top of the cell is a window layer with a band gap of 1.9 eV, and a thickness of 0.05  $\mu\text{m}$ . The quantum well contains 25 layers, each 0.005  $\mu\text{m}$  in thickness with InAs and GaAs semiconductors. The lattice constant for InAs is 6.0584  $\text{\AA}$  and for GaAs is 5.6533  $\text{\AA}$ , Which results in a non-matching of the lattice constant between the two semiconductors in the middle quantum layers. This problem is solved by making thin InAs layers without exceeding the critical thickness 7  $\text{\AA}$ , growing in the direction of 001. Further thicknesses create trap alignments in the structure [17]. Aluminum (0.7%) was added to the  $\text{In}_{0.49}\text{Ga}_{0.51}\text{P}$  to increase the band gap, producing a  $\text{In}_{0.5}(\text{Al}_{0.7}\text{Ga}_{0.3})_{0.5}\text{P}$  semiconductor with a 2.3 eV band gap. Research shows that this semiconductor has a lattice constant matching and GaAs [21-22]. Also,  $\text{In}_{0.5}(\text{Al}_{0.7}\text{Ga}_{0.3})_{0.5}\text{P}$  with creation of an electric field in the EBL and HBL layers reduces recombination of the electrons and holes.

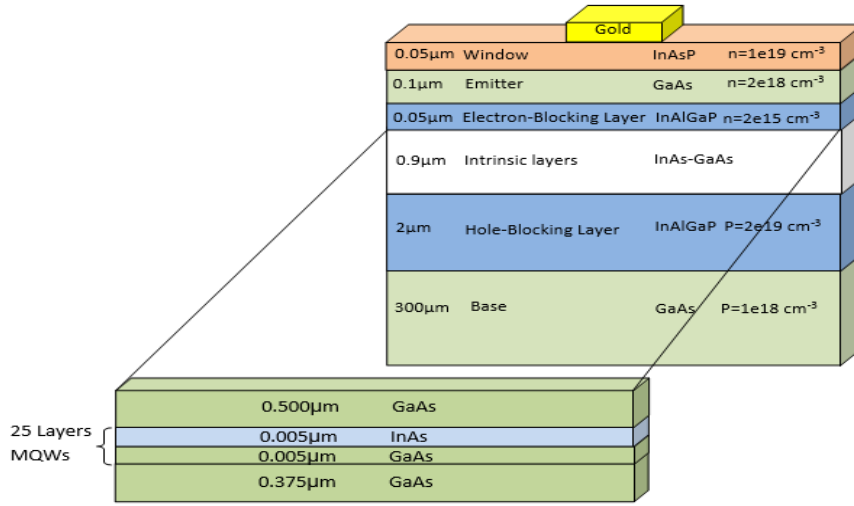


**Fig. 3** Schematic of the proposed cell

##### 4.2. Analysis of proposed model

The current density of the pin solar cell is obtained from Eq. 1:

$$J(V) = J_0(1 + \beta)[\exp(qV/kT) - 1] + J_1[\exp(qV/2kT) - 1] - q\Phi_B \quad (1)$$

where  $K$  is the Boltzmann's constant,  $T$ , the absolute temperature,  $q$ , the electron charge,  $J_0$ , the reverse saturation current densities,  $\Phi_B$  is the net flux of incident photons with energies  $\geq$  band gap energy

$$\beta = \frac{qW_B n_{iB}^2}{J_0} \text{ and } J_1 = qW A_B n_{iB} \quad (2)$$

$\beta$  is the ratio of the current required in the intrinsic region at equilibrium to the usual reverse drift current,  $W$  is intrinsic region width,  $A_B$  is the nonradiative coefficient and  $n_{iB}$

is the equilibrium intrinsic carrier concentration and  $B_B$  is the barrier recombination coefficient.

In Eq. 3, the current to voltage in the solar cell (MQW) is shown [26]:

$$J_{MQW} = J_0(1 + r_R\beta)[\exp(qV/kT) - 1] + (J_1r_{NR} + J_S) \times [\exp(qV/2kT) - 1] - qW\phi \quad (3)$$

where

$$r_R = 1 + f_w[\gamma_B\gamma_{DOS}^2 \exp\{(\Delta E/kT) - 1\}] \text{ and } r_{NR} = 1 + f_w[\gamma_A\gamma_{DOS} \exp\{(\Delta E/2kT) - 1\}] \quad (4)$$

fraction  $f_w$  of the intrinsic region volume substituted by quantum well material  $\gamma_A$  and  $\gamma_B = B_{We}/B_{Ba}$  is the recombination coefficient enhancement factor,  $\gamma_{DOS} = g_{We}/g_{Ba}$  is the effective volume densities of states enhancement factor, and  $\Delta E = E_{Ba} - E_{We}$  Short-circuit current density in pin solar cell (MQW) is obtained from Eq. 5:

$$J_{scQW} = -q[f_\omega N_{ph}(E_{Ba} > E_{We}) + (1 - f_\omega)] \quad (5)$$

Where  $N_{ph}(E_{Ba} > E_{We})$  and  $N_{ph}( > E_{Ba})$  is the net photon flux density corresponding to the energies between  $E_{Ba}$  and  $E_{We}$  for the bulk solar cell. The open circuit voltage in the solar cell pin (MQW) is obtained from Eq. 6 [27]:

$$V_{ocQW} = V_t \ln \left[ \frac{J_s(1+r\beta_1) - J_{scQW}}{J_s(1+r\beta_1)} \right] \quad (6)$$

### 4.3. Model simulation

In this study, the performance of the proposed cell was simulated under the standard AM 1.5 spectrum using Atlas Tcad, and it was segmented by a mesh-structured solar cell with different densities. The CONMOB model was used to calculate the electron and hole excitation capability and to combine the two OPTR and SRH models. The solar cell exposure process was done using the LUMINOUS module [17].

## 5. RESULT AND DISCUSSION

### 5.1. Optimization of thickness and doping in the EBL and HBL layer

Investigating the doping and thickness of  $\text{In}_{0.5}(\text{Al}_{0.7}\text{Ga}_{0.3})_{0.5}\text{P}$  in the EBL and HBL layers of the proposed solar cell is essential for efficient detection. Fig. 4a shows that the highest efficiency for the EBL layer was at a thickness of 0.05  $\mu\text{m}$ . Fig. 4b shows the highest efficiency occurred by adding an EBL layer to a base cell at a doping of  $2 \times 10^{15}$   $1/\text{cm}^3$ . Figs. 5a and 5b show the effect on the thickness and doping of efficiency by adding a HBL layer. Maximum efficiency was achieved at a thickness of 2.0  $\mu\text{m}$  and doping of  $2 \times 10^{19}$   $1/\text{cm}^3$ . It is clear that the addition of  $\text{In}_{0.5}(\text{Al}_{0.7}\text{Ga}_{0.3})_{0.5}\text{P}$  as EBL and HBL layers in the GaAs-based multi-quantum well solar cell as an intermediate layer increased the efficiency 17.38%.

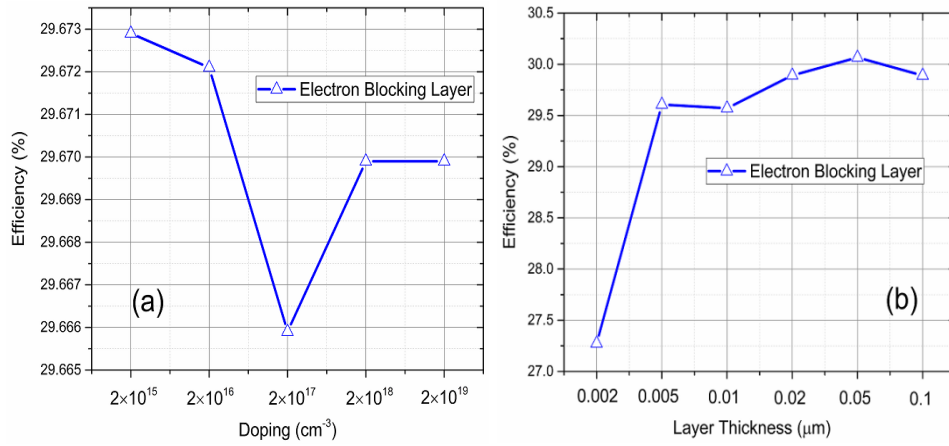


**Fig. 4** a) Different values of the EBL doping (thickness = 0.005(μm)), b) Different values of the EBL thickness (doping = 5 × 10<sup>15</sup>( 1/cm<sup>3</sup>)) ,

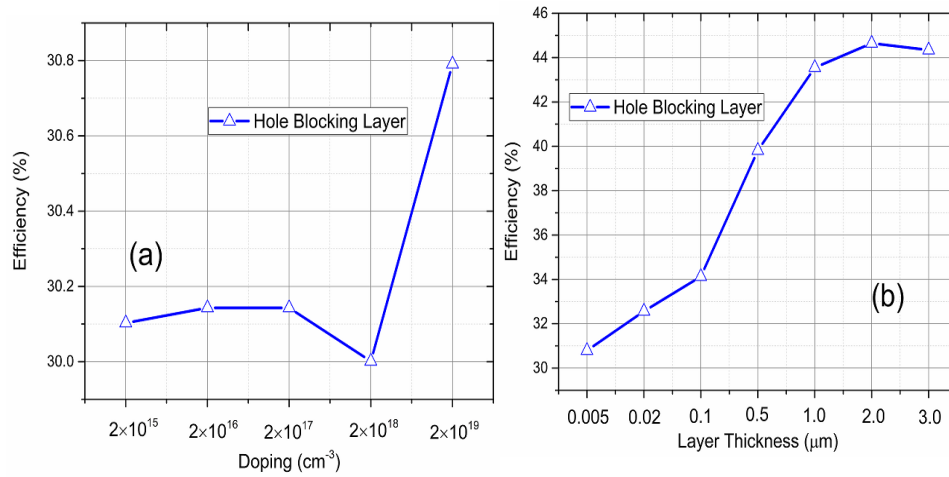


**Fig. 5** a) Different values of the HBL doping (thickness = 0.005(μm )), b) Different values of the HBL thickness (doping = 5 × 10<sup>19</sup>( 1/cm<sup>3</sup>)) .

## 5.2. Electric field

The maximum field at the p-n junction can be calculated using Eq. (7) as:

$$E_m = \frac{qN_D x_n}{\epsilon_s} = \frac{qN_A x_p}{\epsilon_s} \quad (7)$$

Where  $q$  is the Charge of the electron,  $N_A$  is the acceptor impurity density,  $N_D$  is the donor impurity density,  $\epsilon_s$  is the relative dielectric permittivity of the semiconductor,  $x_p$  is the depletion region's width of the p-side, and  $x_n$  is the depletion region's width of the n-side.

The electric field in the junction's region is obtained through Eq. 8 where  $N_B$  is the impurity density in the semiconductor which has widest depletion region.

$$E = \frac{qN_B W}{\epsilon_s} \tag{8}$$

The width of depletion region in a p-n junction can be calculated using Eq. (9) as:

$$W = \sqrt{\frac{2\epsilon_s}{q} \left( \frac{N_A + N_D}{N_A N_D} \right) V_{bi}} \tag{9}$$

where  $V_{bi}$  is the internal potential in both sides of the junction [28]. The in vitro findings of references [29] and [30] were used to conclude that  $In_{0.5}(Al_{0.7}Ga_{0.3})_{0.5}P$  semiconductors increase the open-circuit voltage and the  $V_{bi}$  in the semiconductor. The Eqs. (8) and (9) shows increased the electric field in the region. As seen in Fig. 6, an additional field was created at the interface between the p and EBL layers and the maximum field strength increased from  $2.5 \times 10^4$  to  $2.2 \times 10^5$ . At the interface between the n and HBL layers, the maximum field strength increased from  $3.8 \times 10^4$  to  $6.9 \times 10^5$ , which reduced recombination in the proposed cell.

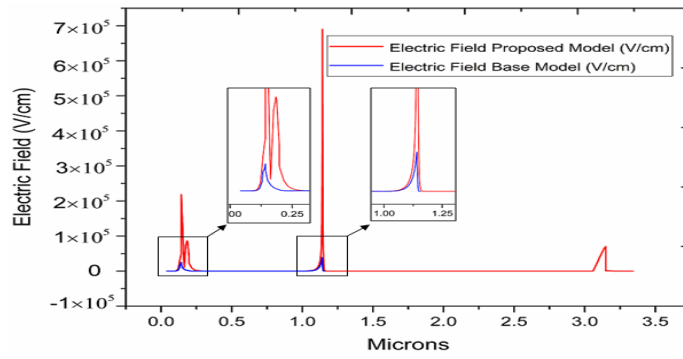


Fig. 6. Maximum electric field at the junction region for base and proposed cell.

### 5.3. Spectral response

The spectral response demonstrates the absorption of photons in a solar cell. Fig. 7 compares the produced and absorbed photons for the base and proposed cells. It can be

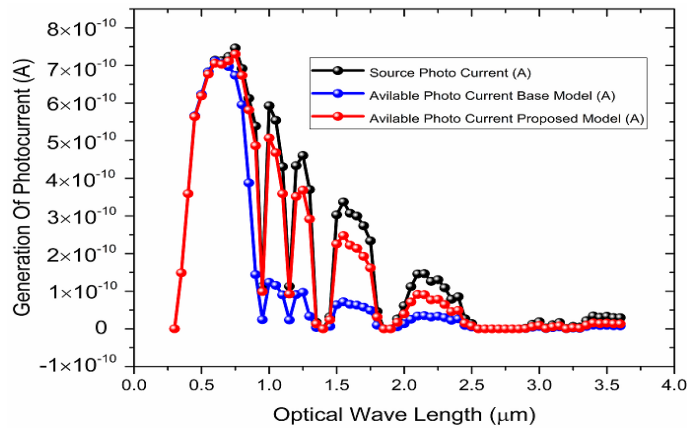


Fig. 7 Generation of photocurrent of the base and proposed cell

observed that the photon absorption rate in the optical spectrum (0.75-2.5  $\mu\text{m}$ ) of the proposed cell is higher than in the base cell, which increases the gain in the proposed cell.

#### 5.4. Photogeneration rate

The photons produced in a solar cell are defined in Eq. (10)

$$G = \eta_0 \frac{P\lambda}{hc} \alpha e^{-\alpha y} \quad (10)$$

In this formula,  $G$  is the Photogeneration rate,  $P$  is the total cumulative effect of reflections, transmissions and losses due to absorption over the ray path,  $y$  is the relative distance for the given ray,  $h$  is the Planck's constant,  $\lambda$  is the wavelength,  $c$  is the speed of light,  $\alpha$  is the absorption coefficient, and  $\eta_0$  is the internal quantum efficiency [31]. The absorption coefficient is obtained from the Eq. (11),  $k$  coefficient has a positive relationship with the absorption coefficient of a material [28]:

$$\alpha(\lambda) = \frac{4\pi k}{\lambda} 10^7 \text{cm}^{-1} \quad (11)$$

Considering Eq. (11) and the investigation of the  $n$  and  $k$  coefficients in AlGaInP semiconductor from reference [28], it can be concluded that by inserting an AlGaInP semiconductor as EBL and HBL, the photogeneration rate will increase. Fig. 8 shows the concordance of the theoretical and simulation results for the proposed cell and the base

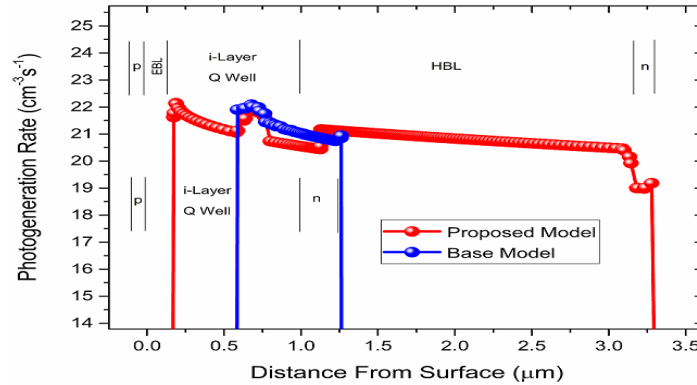
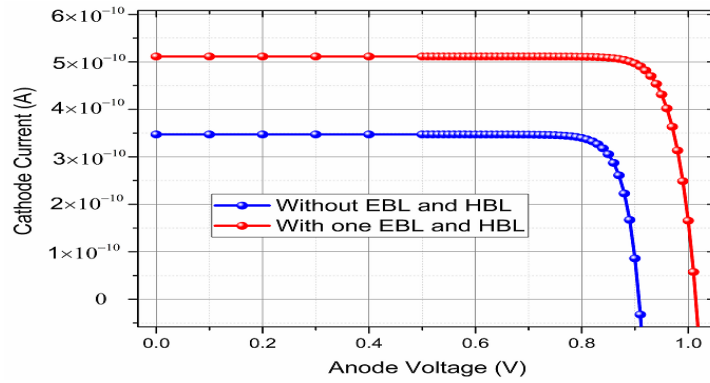


Fig. 8 Photogeneration rate of the base and proposed model

#### 5.5. IV characteristics

Fig. 9 compares the I-V curve of the proposed solar cell with EBL and HBL layers with the base cell without EBL and HBL layers. As seen, the  $\text{In}_{0.5}(\text{Al}_{0.7}\text{Ga}_{0.3})_{0.5}\text{P}$  semiconductor in the EBL and HBL layers decreased recombination, which increased the  $J_{sc}$  and  $V_{oc}$  increased to a value of 0.107 V, compensating for the voltage drop caused by the quantum well layer.



**Fig. 9** Current density-voltage (J-V) characteristics of GaAs-based Multiple Quantum Well solar cells without EBL and HBL, with one EBL and HB

### 5.6. Important parameters in solar cells

Solar cell efficiency can be expressed as shown in Eq. (12) [32].

$$\eta = \frac{P_{\max}}{P_{\text{in}}} = \frac{V_{\text{oc}} I_{\text{sc}} FF}{P_{\text{in}}} \quad (12)$$

where  $P_{\max}$  is the maximum output power,  $P_{\text{in}}$  is the input power and FF is the fill factor.

The total current of a solar cell can be obtained from Eq. (13).

$$I = I_0 \left[ \exp\left(\frac{qV}{nKT}\right) - 1 \right] - I_L \quad (13)$$

$K$  is the Boltzmann constant,  $T$  is the temperature in kelvin,  $I_L$  is the current produced by the photons and  $I_0$  is the current in a dark state.

Short circuit current occurs when  $V = 0$ .  $I_{\text{sc}}$  can be obtained using relation 13 by substituting relation 14. The open circuit voltage is obtained as [33]:

$$I_{\text{sc}} = -I_L \quad (14)$$

for  $I=0$  in Eq. (4) the open circuit voltage and fill factor are calculated in Eqs. (15) and (16).

$$V_{\text{oc}} = \frac{nKT}{q} \ln\left(\frac{I_L}{I_0} + 1\right) \quad (15)$$

$$FF = \frac{V_{\text{oc}} - \ln(V_{\text{oc}} + 0.72)}{V_{\text{oc}} + 1} \quad (16)$$

Table 2 shows the optimized proposed cell model with EBL and HBL layers and base cells without EBL and HBL layers. From the table, it is possible to compare important solar cell parameters such as  $J_{\text{sc}}$ ,  $V_{\text{oc}}$  FF and  $\eta$ .

**Table 2**  $J_{\text{sc}}$ ,  $V_{\text{oc}}$ , FF, and conversion efficiency of multiple quantum well solar cell without EBL and HBL layer, with EBL.

Solar cells	Spectrum	Sun	$V_{\text{oc}}$ (V)	$J_{\text{sc}}$ (mA/cm <sup>2</sup> )	FF (%)	$\eta$ (%)
Without EBL & HBL (25 layers q-well)[11]	AM1.5G	1.0	0.907	34.71	86.63	27.27
With EBL & HBL (25 layers q-well)	AM1.5G	1.0	1.014	51.10	86.20	44.65

## 6. CONCLUSION

In the present study, a  $\text{In}_{0.5}(\text{Al}_{0.7}\text{Ga}_{0.3})_{0.5}\text{P}$  semiconductor as EBL and HBL intermediate layers was added to a GaAs-based 25-layer InAs/GaAs quantum-well solar cell. The impurity density and optimum thickness of the new layers reduced the drop in  $V_{oc}$  caused by the presence of the quantum layers. The optimized cell provides a  $V_{oc}$  of 1.014 V,  $J_{sc}$  of 51.1  $\text{mA}/\text{cm}^2$ , FF of 86.2 % and a conversion efficiency of 44.65% under 1 sun.

## REFERENCES

- [1] K. W. J. Barnham and G. Duggan, "A new approach to high-efficiency multi-band-gap solar cells", *J. Appl. Phys.*, vol. 67, pp. 3490, 1990.
- [2] K. Barnham, B. Braun, J. Nelson, and M. Paxman, "Short-circuit current and energy efficiency enhancement in a low-dimensional structure photovoltaic device," *Appl. Phys. Lett.*, vol. 59, pp. 135–137, 1991.
- [3] M. Paxman, J. Nelson, B. Braun, J. Connolly, and K. W. J. Barnham, "Modeling the spectral response of the quantum well solar cell", *J. Appl. Phys.*, vol. 74, pp. 614, 1993.
- [4] B. P. Rand, J. Li, J. Xue, R. J. Holmes, M. E. Thompson, S. R. Forrest, "Organic Double Heterostructure Photovoltaic Cells Employing Thick Tris(acetylacetonat)ruthenium(III) Exciton-Blocking Layers", *Adv. Mater.*, vol. 17, pp. 2714–2718, 2005.
- [5] Y. K. Kuo, T. H. Wang, J. Y. Chang, J. D. Chen, "Slightly-Doped Step-Like Electron-Blocking Layer in InGaN Light-Emitting Diodes", *IEEE Photonics Technol. Lett.*, vol. 24, no. 17, pp. 1506, 2012.
- [6] M. F. Ali, F. Hossain, "Effect of Bandgap of EBL on Efficiency of the p-n Homojunction Si Solar Cell from Numerical Analysis", In Proceedings of the International Conference on Electrical & Electronic Engineering (ICEEE), 2015, pp. 245–248.
- [7] D. Guimard, R. Morihara, D. Bordel, K. Tanabe, Y. Wakayama, "Fabrication of InAs/GaAs quantum dot solar cells with enhanced photocurrent and without degradation of open circuit voltage", *Applied Physics Letters*, vol. 96, no. 20, pp. 203507, 2010.
- [8] P. J. Carrington, A. S. Mahajumi, M. C. Wagener, J. R. Botha, Q. Zhuang, A. Krier, "Type II GaSb/GaAs quantum dot/ring stacks with extended photoresponse for efficient solar cells", *Physica B: Condensed Matter*, vol. 407, no. 10, pp. 1493–1496, 2012.
- [9] W. S. Liu, H. M. Wu, F. H. Tsao, T. L. Hsu, J. I. Chyi, "Improving the characteristics of intermediate-band solar cell devices using a vertically aligned InAs/GaAsSb quantum dot structure", *Solar Energy Materials & Solar Cells*, vol. 105, pp. 237–241, 2012.
- [10] X. Yang, K. Wang, Y. Gu, H. Ni, X. Wang, T. Yang, Z. Wang, "Improved efficiency of InAs/GaAs quantum dots solar cells by Si-doping", *Solar Energy Materials & Solar Cells*, vol. 113, pp. 144–147, 2013.
- [11] Y. Dai, S. Polly, S. Hellstroem, D. V. Forbes and S. M. Hubbard, "Electric Field Effect on Carrier Escape from InAs/GaAs Quantum Dots Solar cells", In Proceedings of the IEEE 40th Photovoltaic Specialist Conference (PVSC), 2014, pp. 3492–3497.
- [12] I. Ramiro, J. Villa, P. Lam, S. Hatch, J. Wu, E. Lopez, E. Antolín, H. Liu, A. Mart ,Wide-Bandgap InAs/InGaP Quantum-Dot Intermediate Band Solar Cells, *IEEE Journal of Photovoltaics*, vol. 5 , no. 3, pp. 840–845, 2015.
- [13] A. D. Utrilla, D. F. Reyes, J. M. Llorens, I. Artacho, T. Ben, D. González, Ž. Gačević, A. Kurtz, A. Guzman, A. Hierro, J. M. Ulloa, "Thin GaAsSb capping layers for improved performance of InAs/GaAs quantum dot solar cells", *Solar Energy Materials and Solar Cells*, vol. 159, pp. 282–289, 2017.
- [14] S. Biswas and A. Sinha, "An analytical study of the minority carrier distribution and photocurrent of a p–i–n quantum dot solar cell based on the InAs/GaAs system", *Indian Journal of Physics*, vol. 91, pp. 1197–1203, 2017
- [15] A. Imran, J. Jiang, D. Eric, M. N. Zahid, M. Yousaf, Z. H. Shah, "Optical properties of InAs/GaAs quantum dot superlattice structures", *Results in Physics*, vol. 9, pp. 297–302, 2018.
- [16] A. Aissat, N. Harchouch, and J. P. Vilcot, "Optimization of the Temperature Effects on Structure InAs/GaAs QDSC", In: Hajji B., Tina G., Ghoumid K., Rabhi A., Mellit A. (eds), In Proceedings of the 1st International Conference on Electronic Engineering and Renewable Energy. ICEERE 2018. Lecture Notes in Electrical Engineering, Vol. 519. Springer, Singapore, 2019.
- [17] E. Koletsios, GaAs/InAs multi quantum well solar cell, master of science in applied physics from the naval Postgraduate school, 2012.

- [18] K. J. Singh, S. K. Sarkar, “Highly efficient ARC less InGaP/GaAs DJ solar cell numerical modeling using optimized InAlGaP BSF layers”, *Optical Quantum Electronics*, vol. 43, pp. 1–21, 2012.
- [19] A. Marti, C. R. Stanley, and A. Luque. “Intermediate Band Solar Cells (IBSC) Using Nanotechnology”, chapter 17 in *Nanostructured Materials for Solar Energy Conversion*. (Elsevier B. V., 2006).
- [20] F. K. Rault, “Mathematical Modelling of the Refractive Index and Reflectivity of the Quantum Well Solar Cell”, chapter 4 in *Nanostructured Materials for Solar Energy Conversion*. (Elsevier B. V., 2006).
- [21] Ching-Hwa Ho, Ji-Han Li, and Yu-Shyan Lin, “Optical characterization of a GaAs/In<sub>0.5</sub>(Al<sub>x</sub>Ga<sub>1-x</sub>)<sub>0.5</sub>P/GaAs heterostructure cavity by piezoreflectance spectroscopy”, *Optics Express*, vol. 15, no. 21, pp. 13886–13893, 2007.
- [22] I. Vurgaftman, J.R. Meyer, L.R. Rammohan, “Band parameters for IIIeV compound semiconductors and their alloys”, *J. Appl. Phys.*, vol. 89, no. 11, pp. 5815, 2001.
- [23] SILVACO Data Systems Inc, Silvaco ATLAS User’s Manual, 2010.
- [24] H.Y. Lee, C.T. Lee, “The investigation for various treatments of InAlGaP Schottky diodes”, In *Proceedings of the 8th International Conference on Electronic Materials, IUMRS-ICEM 23, 2002*, pp. 99–102.
- [25] A. Badea, F. Dragan, L. Fara, and P. Sterian, “Quantum mechanical effects analysis of nanostructured solar cell models”, *Renew. Energy Environ. Sustain.*, vol. 1, no. 3, pp. 1–5, 2016.
- [26] J. C. Rimada and L. Hernández, “Modelling of ideal AlGaAs quantum well solar cells”, *Microelectronics Journal*, vol. 32, no. 9, pp. 719–723, 2001.
- [27] G. Siddharth, V. Garg, B. S. Sengar, R. Bhardwaj, P. Kumar, S. Mukherjee, “Analytical Study of Performance Parameters of InGaN/GaN Multiple Quantum Well Solar Cell”, *IEEE Transactions on Electron Devices*, vol. 66, no. 8, pp. 3399–3404, 2019.
- [28] S. Abbasian, R. sabbaghi-Nadooshan, “Design and evaluation of ARC less InGaP/AlGaInP DJ solar cell”, *Optik*, Vol. 136, pp. 487-496, 2017
- [29] E. E. Perl, J. Simon, J. F. Geisz, W. Olavarria, M. Young, A. D. Daniel, J. Friedman, M. A. Steiner, “Development of High-Bandgap AlGaInP Solar Cells Grown by Organometallic Vapor-Phase Epitaxy”, *IEEE Journal of Photovoltaics*, vol. 6, no. 3, pp. 770–776, 2016.
- [30] X. Li, W. Zhang, J. Zhang, H. Lu, D. Zhou, L. Sun, K. Chen, “Study on 2.05 eV AlO<sub>1.3</sub>GaInP sub-cell and its hetero-structure cells”, In *Proceedings of the 40th Photovoltaic Specialist Conference (PVSC)*, 2014, pp. 479–481.
- [31] S. Abbasian, R. Sabbaghi-Nadooshan, “Introducing a novel high-efficiency ARC less heterojunction DJ solar cell”, *Facta Universitatis, Series: Electronics and Energetics*, vol. 31, no. 1, pp. 89–100, 2018.
- [32] S. M. SZE, M. K. LEE. *Semiconductor Devices Physics and Technology*,
- [33] J. P. Dutta, P. P. Nayak, G. P. Mishra, “Design and evaluation of ARC less InGaP/GaAs DJ solar cell with InGaP tunnel junction and optimized double top BSF layer”, *Optik*, vol. 127, pp. 4156–4161, 2016.